CHEMISTRY OF MATERIALS

ARTICLE

pubs.acs.org/cm

Lithium Migration at High Temperatures in $Li_4Ti_5O_{12}$ Studied by Neutron Diffraction

Andreas Laumann,*[,†] Hans Boysen,[‡] Martin Bremholm,[§] K. Thomas Fehr,[†] Markus Hoelzel,[⊥,¶] and Michael Holzapfel[∥]

[†]Department für Geo- und Umweltwissenschaften, Sektion für Mineralogie, Petrologie und Geochemie, LMU München, Theresienstrasse 41, 80333 München, Germany

[‡]Department für Geo- und Umweltwissenschaften, Sektion Kristallographie, LMU München, Am Coulombwall 6, 85748 Garching, Germany

[§]Department of Chemistry, Princeton University, Washington Road, Princeton, New Jersey 08544, United States

[⊥]Fachbereich Material- und Geowissenschaften, Fachgebiet Strukturforschung, Technische Universität Darmstadt, Petersenstrasse 23, 63762 Darmstadt, Germany

[¶]Forschungsneutronenquelle FRM II, Technische Universität München, Lichtenbergstrasse 1, 85747 Garching, Germany

[∥]Battery Materials, Süd-Chemie AG, Ostenrieder Strasse 15, 85368 Moosburg, Germany

Supporting Information

ABSTRACT: The structure of $Li_4Ti_5O_{12}$ was investigated by neutron powder diffraction, and the study revealed unprecedented details about lithium migration at high temperatures. A commercial sample of the battery anode material $Li_4Ti_5O_{12}$ (spinel-type) was measured from room temperature to 1100 °C. Up to 500 °C, linearly increasing values for the unit cell parameter, the isotropic atomic displacement parameters, and the oxygen position are observed. At 700 °C, a change of slope occurs, which is assigned to the beginning migration of lithium. Previous investigations identified the octahedral 16c site in the spinel structure as the migration position of lithium upon heating to high temperatures, and because of that, several phase transitions of $Li_4Ti_5O_{12}$ at high temperatures have been proposed. Here, we unambiguously identify that the lithium atoms occupy split sites around the 16c positions and order−disorder phase transitions of $Li_4Ti_5O_{12}$ were not observed. One-particle potential shows that the occupancy of 16c is an unstable configuration and that the split-site structure leads to a more favorable migration position. Occupation of the lithium sites (32e) results in the same long-range diffusion path in all ⟨110⟩ directions. The onset of lithium migration can explain the change of the ionic conductivity of $Li_4Ti_5O_{12}$ at high temperatures, which has been observed by impedance spectroscopic studies. Further heating to 1000 °C resulted in a partial decomposition of $Li_4Ti_5O_{12}$ into the ramsdellite-type $Li_2Ti_3O_7$ and the cubic γ-Li_2TiO_3, and at 1100 °C, the $Li_4Ti_5O_{12}$ spinel was fully decomposed.

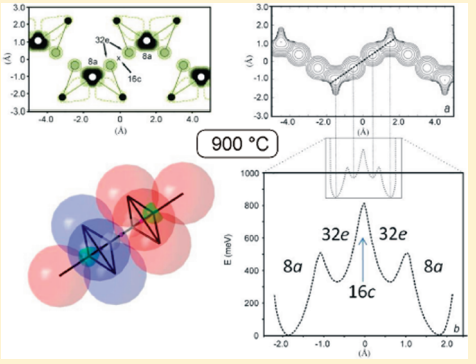

KEYWORDS: $Li_4Ti_5O_{12}$, lithium-ion batteries, neutron diffraction, lithium migration, decomposition

INTRODUCTION

In the current efforts to develop and produce active materials for long-life lithium-ion batteries, e.g., for electronic vehicles or stationary power plants, the anode material $Li_4Ti_5O_{12}$ is a very promising candidate because of its long-term stability at high capacity and its inherent safety.[1−6] Its spinel structure of space group $Fd\bar{3}m$ was determined by Deschanvres et al.[7] and recently reinvestigated by single-crystal X-ray diffraction.[8] Its unit cell contains eight formula units of $(Li)^{8a}[Li_{1/3}Ti_{5/3}]^{16d}O_4{}^{32e}$, in which lithium fully occupies the tetrahedral 8a sites. The octahedral 16d sites are occupied randomly by lithium atoms ($^1/_6$) and titanium atoms ($^5/_6$),[8,9] and the oxygen atoms are on the 32e sites.[2,8] With a theoretical specific capacity of 175 mAh/g, three Li^+ ions can be intercalated electrochemically in $Li_4Ti_5O_{12}$ at a flat potential of 1.55 V. During lithiation, lithium shifts from tetrahedral 8a sites toward the octahedral 16c sites $[(Li)_{1-x}{}^{8a}[Li]_{2x}{}^{16c}[Li_{1/3}Ti_{5/3}]^{16d}O_4{}^{32e}]$, causing only minor structural strain ("zero strain material"), which is ascribed to enable the excellent cyclability of $Li_4Ti_5O_{12}$.[2,3,10−12]

Upon heating of the $Li_4Ti_5O_{12}$ samples, variations of its activation energy were determined by impedance spectroscopy,[13−16] which have been assigned to structural changes of the order−disorder type.[13−15] Similar conclusions were reported based on data obtained by IR spectroscopy,[17] Raman spectroscopy,[14] and NMR spectroscopy.[18] Following the impedance data, $Li_4Ti_5O_{12}$ is presumed to undergo two order−disorder phase transitions

Received: November 20, 2010
Revised: April 5, 2011
Published: May 03, 2011

upon heating. The first transition is due to migration of lithium from 8a to 16c sites and the transition to an ordered NaCl type structure with $Fd\bar{3}m$ structure ($[Li]^{16c}[Li_{1/3}Ti_{5/3}]^{16d}O_4^{32e}$), and the second transition is due to migration of lithium from 16d to 16c sites, transforming it into a disordered NaCl structure with $Fm\bar{3}m$ ($[Li_{4/3}]^{16c}[Ti_{5/3}]^{16d}O_4^{32e}$).[13,14] All proposed structural transformations are well below the decomposition temperature of $Li_4Ti_5O_{12}$ into the ramsdellite-type $Li_2Ti_3O_7$ and the cubic Li_2TiO_3 at approximately 1000 °C.[19−21] However, inconsistencies about the lithium distribution in $Li_4Ti_5O_{12}$ are also reported at room temperature. Contrary to the most common opinion in the literature, a partial occupation of 16c octahedral positions due to migration of tetrahedrally bound lithium to interstitial sites has been proposed[13,14] and shown by NMR spectroscopy[18] and an IR spectroscopy study[17] at room temperature.

A lithium diffusion path of $Li_4Ti_5O_{12}$ at room temperature, 8a → 16c → 8a or 8a → 16c → 48f → 16d, and direct lithium hopping between 16c and 16d or 8a and 48f have been proposed,[22] whereas in the recent publication of Wagemaker et al.,[23] the 16c octahedral position was identified as the saddle point of the energy barrier between two tetrahedral 8a sites. The latter results in a negligible occupation time of lithium on 16c when hopping from one 8a to another 8a.

Neutron powder diffraction has so far mainly been applied to study the lithium intercalation process in $Li_4Ti_5O_{12}$.[10−12,24] The aim of the present study was to elucidate the structural changes and diffusion properties during stepwise heating up to 1100 °C. An increase in the lithium-ion mobility was found starting at approximately 700 °C and analyzed in detail at 900 °C. Phase transitions of the order−disorder type were not observed. Decomposition of $Li_4Ti_5O_{12}$ to $Li_2Ti_3O_7$ and cubic γ-Li_2TiO_3 started at 1000 °C, leading to complete decomposition at 1100 °C.

EXPERIMENTAL SECTION

The $Li_4Ti_5O_{12}$ powder used was a commercial compound provided by Süd-Chemie AG, Moosburg, Germany. Preliminary laboratory powder X-ray diffraction (PXRD) characterization [STOE STADI P, Cu Kα_1 radiation, λ = 1.544 056 Å, curved Ge(111) monochromator] showed a pure phase.

Neutron powder diffraction measurements were carried out on a high-resolution SPODI diffractometer[25] at FRM II (Garching, Germany). The wavelength, λ, was determined from the measurement of a silicon standard (NIST SRM 640c) to be 1.5483 Å. For multitemperature measurements, a niobium container was filled with 2 g of the commercial $Li_4Ti_5O_{12}$ powder and placed in a high-temperature vacuum furnace. The reflections from niobium were included in all refinements. Diffraction patterns were collected at room temperature, 300, 500, 700, 900, 1000, and 1100 °C. Additional patterns were recorded after cooling to 700 °C and further to room temperature. Each data set was collected for 2 h after a holding time of 15 min for temperature equilibration. The neutron powder patterns were recorded from 0.95° to 160° 2θ with a step size of 0.05°. Rietveld refinement was performed using the program *FullProf*.[26] The pseudo-Voigt function in the formulation of Thompson−Cox−Hastings[27] was used to model the line shape. The background was linearly interpolated between a set of background points with refinable intensities. Additional refinements, including anharmonic terms in the Debye−Waller factor, were performed using the program *JANA*.[28]

RESULTS

The structure refinement of $Li_4Ti_5O_{12}$ was performed following the convention of most of the previous literature on this compound (e.g., refs 8,12, and 22), i.e., using the second setting of the space group $Fd\bar{3}m$ in the International Tables of Crystallography[29] with the symmetry center at the origin and Li1 on 8a ($^1/_8\ ^1/_8\ ^1/_8$), Ti/Li2 on 16d ($^1/_2\ ^1/_2\ ^1/_2$), and O on 32e ($x\ x\ x$) sites. Here x is close to $^1/_4$ and is often written as $x = {}^1/_4 + u$. The small value of u determines the relative size of the tetrahedra and octahedra; a positive value increases the tetrahedral volume. The bond lengths Li1−O and Ti/Li2−O are equal at $u = {}^1/_{80}$. For standard refinements, lithium was fixed to full occupancy on 8a sites and to $^1/_6$ occupancy on 16d sites and titanium to $^5/_6$ on 16d sites, as reported before.[8,12,24]

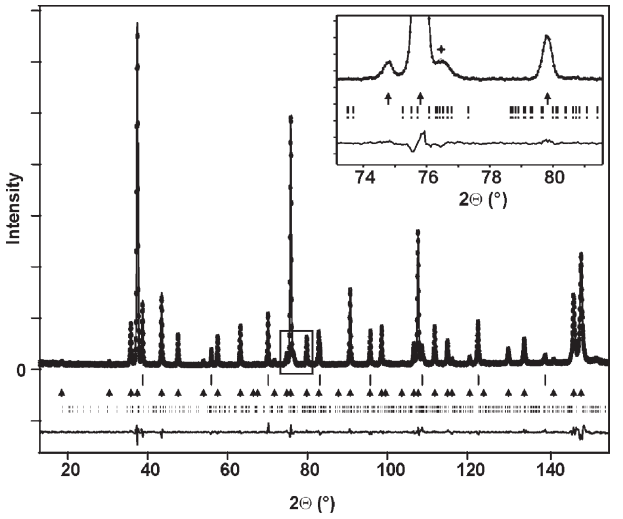

Figure 1. Rietveld fit of $Li_4Ti_5O_{12}$ at room temperature. Observed (circles) and calculated (solid line) patterns, Bragg reflections of niobium (solid ticks), $Li_4Ti_5O_{12}$ (arrows), β-Li_2TiO_3 (dashed ticks), and the difference curve (below) are shown. The asterisk in the inset marks the only obvious group of reflections of β-Li_2TiO_3 that are not superposed by $Li_4Ti_5O_{12}$ peaks.

The spinel $Li_4Ti_5O_{12}$ was refined in space group $Fd\bar{3}m$ with a unit cell parameter of a = 8.35952(4) Å at 15 °C, showing good agreement with reported values, e.g., a = 8.352(4) Å[8] and a = 8.35950 Å[3] (Figure 1). A minor impurity phase of monoclinic Li_2TiO_3 (β-Li_2TiO_3) was found to be present <3 wt %, but could not be detected by PXRD. The structure of β-Li_2TiO_3 is described as pseudocubic, leading to similar neutron powder and PXRD patterns of β-Li_2TiO_3 and $Li_4Ti_5O_{12}$, and as such, nearly all reflections of β-Li_2TiO_3 with higher intensity are superimposed by reflections of the major phase $Li_4Ti_5O_{12}$. Only one group of reflections at approximately 77° 2θ clearly indicates the presence of β-Li_2TiO_3 (see the inset of Figure 1). All other β-Li_2TiO_3 reflections either are too low in intensity or only cause peak broadening or weak shoulders on $Li_4Ti_5O_{12}$ reflections. The low content does not allow a structural refinement of β-Li_2TiO_3, and therefore the structural values of Kataoka et al.[30] were used. The impurity of β-Li_2TiO_3 was within uncertainties constant up to 700 °C. At 900 °C, no clear reflection of β-Li_2TiO_3 could be detected.

Neutron Diffraction Measurements upon Heating and Cooling of the $Li_4Ti_5O_{12}$ Sample. Up to 700 °C, the unit cell parameter (Figure 2a), the u parameter of oxygen (Figure 2b), the Li1−O (tetrahedra) and Li2/Ti−O (octahedra) bond distances (Figure 2c), and all isotropic thermal displacement parameters B_{iso} (Figure 2d) increased in a near-linear manner (Table 1). At higher temperatures and as is clearly seen at 900 °C,

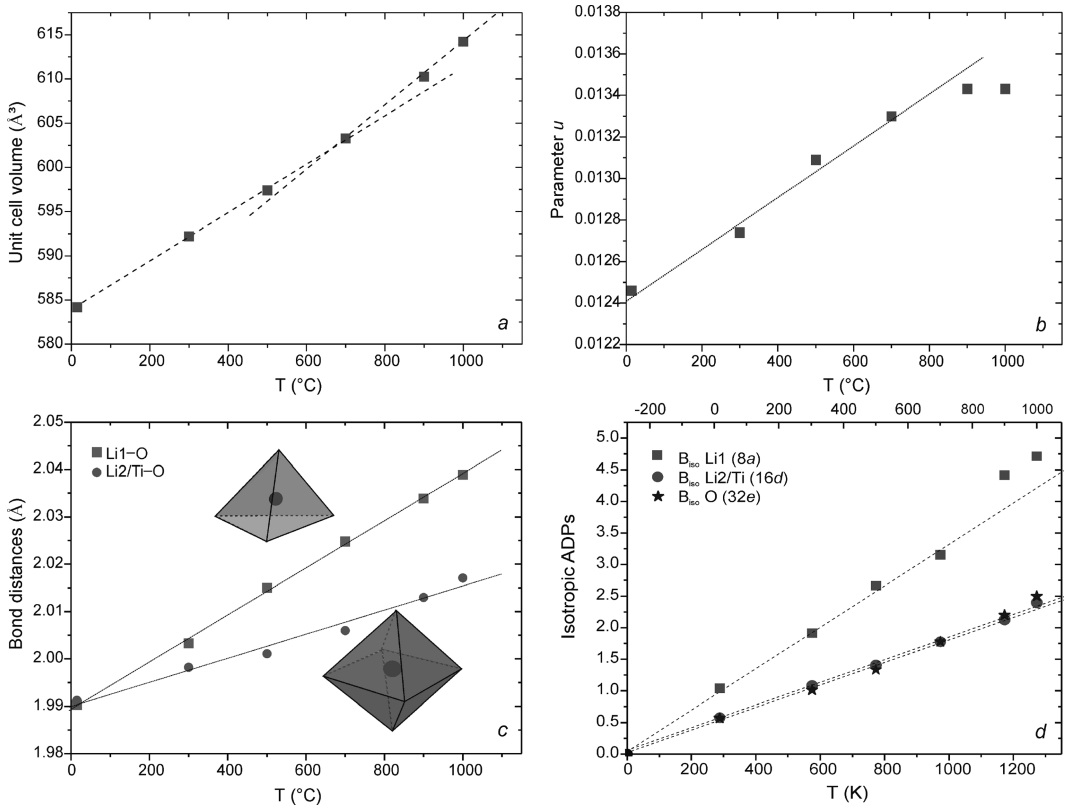

Figure 2. Structural evolution of $Li_4Ti_5O_{12}$ upon heating: (a) the unit cell volume with linear fits for $T < 700$ °C and > 700 °C, (b) the parameter u, (c) selected bond distances, and (d) the isotropic ADPs (the straight lines are fitted to the values below 900 °C passing through 0 K).

Table 1. Structural Parameters of $Li_4Ti_5O_{12}$ at Varying Temperatures[a]

	temp (°C)					
	15	300	500	700	900	1000
a (Å)	8.35956(3)	8.39766(5)	8.42219(5)	8.44977(6)	8.48218(5)	8.50051(6)
V (Å^3)	584.186(4)	592.208(6)	597.413(6)	603.301(5)	610.270(7)	614.236(7)
u	0.01246(3)	0.01273(4)	0.01313(4)	0.01335(3)	0.01344(4)	0.01348(5)
B_{iso} Li (8a)	1.02(7)	1.90(11)	2.66(13)	3.11(11)	4.44(17)	4.76(19)
B_{iso} Li/Ti (16d)	0.62(2)	1.21(3)	1.38(3)	1.74(3)	2.12(3)	2.36(4)
B_{iso} O (32e)	0.59(1)	1.07(2)	1.34(2)	1.75(1)	2.22(2)	2.50(2)
R_p	4.70	5.48	4.94	3.68	4.13	3.83
R_{wp}	5.63	6.59	6.10	4.67	5.27	4.96
χ^2	2.74	1.91	1.63	1.91	2.52	1.82

[a] Number of data points: 3138. Number of refined background parameters: 52 (46 at 1000 °C). Total number of refined parameters: 78 (73 at 1000 °C).

these parameters, except the bond distances, show deviations from linearity, which will be discussed in detail below.

At 1000 °C, $Li_4Ti_5O_{12}$ started to decompose into the ramsdellite-type phase $Li_2Ti_3O_7$ and the cubic Li_2TiO_3 (γ-Li_2TiO_3), with fractions, excluding niobium, of 3.18(4) and 1.29(7) wt %, respectively. Monoclinic β-Li_2TiO_3 undergoes an order−disorder transformation at high temperatures to the cubic γ-Li_2TiO_3: for compositions Li/Ti ∼ 2, the transformation temperature is approximately 1150 °C.[20,30] Lower Li/Ti ratios are reported to reduce the transformation temperature.[19−21]

At 1100 °C, $Li_4Ti_5O_{12}$ had fully decomposed into $Li_2Ti_3O_7$ and γ-Li_2TiO_3 in a fractional ratio of 2.61(2):1 wt % (Table 2 and Figure 3). At 1100 °C, γ-Li_2TiO_3 has a unit cell parameter of $a = 4.24394(4)$ Å, which is close to a previously reported value at the same temperature, $a = 4.23929(10)$ Å.[31]

Upon cooling to 700 °C, the γ-Li_2TiO_3 phase did undergo the expected transformation to the stable β-Li_2TiO_3. To conserve the ramsdellite-type structure of $Li_2Ti_3O_7$, the compound must be quenched rapidly to room temperature.[32] Slow cooling of $Li_2Ti_3O_7$ will result in its decomposition to $Li_4Ti_5O_{12}$ and TiO_2. At 700 °C and at room temperature, besides $Li_2Ti_3O_7$ and the β-Li_2TiO_3, $Li_4Ti_5O_{12}$ reappeared with a fraction of ∼15 wt %, and a minor fraction of rutile (<1 wt %) was detected at room temperature. The temperature-dependent progression upon heating of the $Li_4Ti_5O_{12}$ sample to its decomposition starting at 1000 °C is presented in Figure 4.

dx.doi.org/10.1021/cm103332y |Chem. Mater. 2011, 23, 2753–2759

Table 2. Structural Parameters of γ-Li_2TiO_3 and $Li_2Ti_3O_7$ at 1100 °C[a]

compound	γ-Li_2TiO_3	$Li_2Ti_3O_7$
a (Å)	4.24394(4)	5.09801(6)
b (Å)		9.7095(1)
c (Å)		2.98604(3)
V (Å^3)	76.438(1)	147.805(3)
composition (%)[b]	27.74(2)	72.25(3)
R_F (%)	3.5	6.64

[a] Number of data points: 3138. Number of refined background parameters: 46. Total number of refined parameters: 72. R_p: 3.68. R_{wp}: 4.63. χ^2: 1.78. [b] Niobium content excluded.

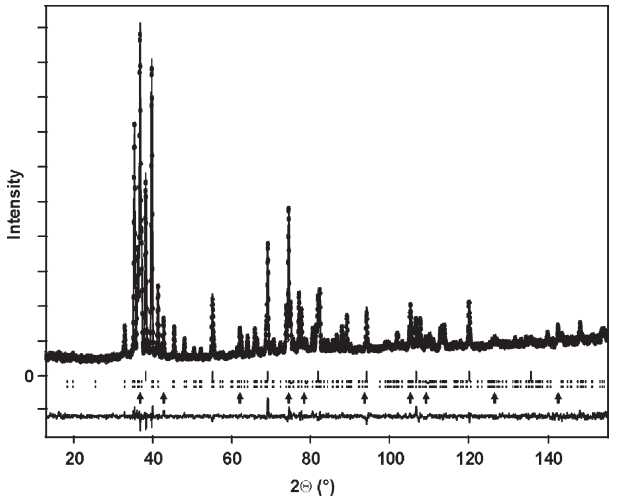

Figure 3. Rietveld fit of the decomposition products $Li_2Ti_3O_7$ and γ-Li_2TiO_3 at 1100 °C. Observed (circles) and calculated (solid line) pattern intensities, Bragg reflections of niobium (solid ticks), $Li_2Ti_3O_7$ (dashed ticks), cubic γ-Li_2TiO_3 (arrows), and the difference curve (below) are shown.

Lithium Migration at High Temperatures. As mentioned above, the unit cell volume, the oxygen position (parameter u), and the isotropic thermal displacement parameter B_{iso} of Li1 on 8a deviated significantly from a linear trend at high temperatures. Therefore, test refinements following the proposal of Leonidov et al.[13,14] were performed, with lithium either partially or fully on 16c instead of 8a or with all lithium on 16c ($[Li_{4/3}]^{16c}[Ti_{5/3}]^{16d}O_4{}^{32e}$) either in space group $Fd\bar{3}m$ or in space group $Fm\bar{3}m$. All of these attempts were unsuccessful and, especially, $^4/_3$ of lithium on 16c can be completely ruled out.

On the contrary, remaining in space group $Fd\bar{3}m$, refinements of the lithium occupancy on 8a at higher temperatures enabled stable fits and showed increasing lithium deficits with increasing temperature. Confirming full occupancy at low temperatures, at 700 °C, the refinement revealed a small deficit, slightly larger than the error margin [0.97(2)], suggesting almost full occupancy, but at 900 °C, a striking decrease of ~14% toward 0.86(2) was revealed. This apparent lithium deficit is not due to evaporation of lithium (see the later discussion) but can be assigned to anharmonic motions and/or migration to other sites in the structure. This could be shown by additional refinements using the program *JANA*,[28] which allows the inclusion of anharmonic terms in the Debye–Waller factor. Note that the

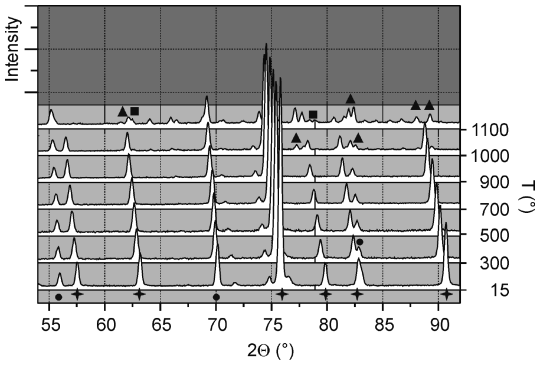

Figure 4. Diffraction patterns (2θ range, 54–92°) as a function of the temperature, with the marked main reflections of $Li_4Ti_5O_{12}$ (asterisks), $Li_2Ti_3O_7$ (triangles), γ-Li_2TiO_3 (squares), and niobium (circles). The partial decomposition of $Li_4Ti_5O_{12}$ into $Li_2Ti_3O_7$ and γ-Li_2TiO_3 can be seen at 1000 °C, and at 1100 °C, $Li_4Ti_5O_{12}$ is fully decomposed.

local symmetry of $\bar{4}3m$ only allows one isotropic harmonic displacement parameter (ADP). There are one third-order term, c^{123}, and two fourth-order terms, d^{1111} and d^{1122}. While c^{123} turned out to be highly significant, the other two were less reliable and produced some artifacts, and thus only c^{123} was used in the following refinements. During these refinements, the lithium occupancy on 16d was kept constant. A subsequent difference Fourier analysis revealed weak but significant negative residual densities within the 16c octahedron (note that the scattering length of lithium is negative). This was found as two peaks along the *xxx* direction displaced from the central 16c position. Therefore, a new atom Li* was introduced on a 32e site. A free refinement of both the occupancy and an isotropic ADP (U_{iso} of Li*) was unsuccessful because of the usually strong correlation between these two parameters, in particular for the very low occupancy. Therefore, U_{iso} was constrained to that of Li1. Free refinement of the occupancies of Li1 and Li* gave values such that the overall sum was conserved within the rather large standard uncertainties, and so, in the final refinement, the overall occupancy was fixed. The results are given in Table 3 and selected bond lengths in Table 4. It should be added that similar refinements at lower temperatures were unsuccessful because of the lower occupancy of the Li* site, and at higher temperatures, the results might be influenced by the gradual onset of the $Li_4Ti_5O_{12}$ decomposition (see above).

Although these results should not be taken too literally because of the necessary constraints, the general distribution of lithium can be deduced with confidence. The corresponding probability density function (PDF) as derived from the ADPs is shown in Figure 5. Assuming Boltzmann statistics for single particle motion, a one-particle potential (OPP) can be deduced. In such OPP maps, the saddle points may be interpreted as activation energies of ion diffusion (for details, see, e.g., ref 33). Figure 6a shows the two-dimensional potential landscape, and Figure 6b shows a one-dimensional section along [111].

DISCUSSION

Composition and Phase Relations of $Li_4Ti_5O_{12}$. Refinements from room temperature up to 700 °C showed a constant ratio of $Li_4Ti_5O_{12}$ and β-Li_2TiO_3. At room temperature, these two phases are immiscible and mixtures of both are common when having lithium in excess; see, e.g., refs 2 and 34. At 900 °C, a

Table 3. Structural Parameters for $Li_4Ti_5O_{12}$ at 900 °C with a Li* 32e Site Included: Fractional Atomic Coordinates and Isotropic or Equivalent Isotropic Displacement Parameters (Å^2), as Well as the Anisotropic and Anharmonic ADPs of Li1 and O

	x	y	z	U_{iso}*/U_{eq}	occupacy
Li1 (8a)	0.125	0.125	0.125	0.037(1)*	0.86(2)
Li2 (16d)	0.5	0.5	0.5	0.0271(5)*	0.1667
Ti (16d)	0.5	0.5	0.5	0.0271(5)*	0.8333
O (32e)	0.26299(5)	0.26299(5)	0.26299(5)	0.02787(13)	1
Li* (32e)	0.043(8)	0.043(8)	0.043(8)	0.037(1)*	0.034(6)
Anisotropic and Anharmonic ADPs					
Li1			$c^{123} = -0.007(2)$		
O			$U_{11} = U_{22} = U_{33} = 0.0279(2)$ Å^2, $U_{12} = U_{13} = U_{23} = -0.0044(2)$ Å^2		

Table 4. Selected Bond Lengths (Å) of $Li_4Ti_5O_{12}$ at 900 °C

Li1−O (4×)	2.0272(5)	Li*−O1 (3×)	1.98(7)
Li1−Li* (4×)	1.20(7)	Li*−O1 (3×)	2.62(7)
Li1−Li* (4×)	2.47(7)	Li*−Li* (1×)	1.28(10)
Ti/Li2−O (6×)	2.0164(5)	Li*−Li* (3×)	1.96(10)

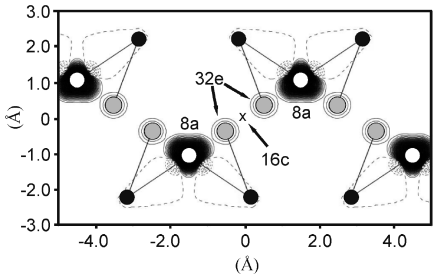

Figure 5. PDF of lithium at 900 °C in the *xxz* plane through 8a and 16c sites. The shortest bond distances between lithium [Li on 8a (white), Li* on 32e (gray), and O on 32e (black)] are indicated. Long dashed lines indicate zero densities and short dashed lines negative densities.

rather homogeneous phase was found to be present and the β-Li_2TiO_3 impurities were <0.5 wt %. Vtiņš et al. mentioned that mixtures of $Li_4Ti_5O_{12}$ and β-Li_2TiO_3 form solid solutions of $Li_{2-x}Ti_{1+x}O_3$ above 900 °C.[15] For our sample, either the annealing for 2 h at 900 °C was too short or the temperature was too low to obtain a complete solid solution and therefore still a minor fraction of β-Li_2TiO_3 was detected.

Decomposition of the $Li_4Ti_5O_{12}$ sample started at 1000 °C, which is within the reported range.[19,20] At 1100 °C, the spinel had fully decomposed into the ramsdellite-type $Li_2Ti_3O_7$ and γ-Li_2TiO_3. The ratio of $Li_2Ti_3O_7$ to γ-Li_2TiO_3 of 2.61(2):1 at 1100 °C equals a Li/Ti ratio of 0.82(1):1, which is ∼2% higher than the Li/Ti ratio in $Li_4Ti_5O_{12}$. Considering the minor β-Li_2TiO_3 fraction at low temperature, the Li/Ti ratio is rather stable during the whole experiment and no sign of lithium evaporation was noticeable. Therefore, e.g., the usage of 8% lithium in excess for the syntheses of $Li_4Ti_5O_{12}$ to compensate for the lithium loss at high temperatures[1] and similar assumptions in refs 35 and 36 should be considered with care. A plausible explanation for using lithium in excess might be the similarity of the diffraction patterns of $Li_4Ti_5O_{12}$ and β-Li_2TiO_3. Minor impurities of β-Li_2TiO_3 are hard to detect by standard PXRD, whereas only a slight lithium deficiency in $Li_4Ti_5O_{12}$ causes clear reflections of titania.

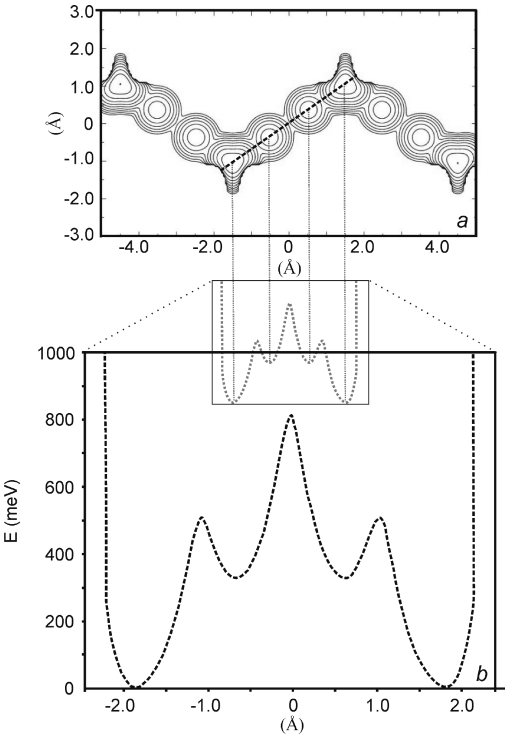

Figure 6. (a) OPP of lithium at 900 °C in the *xxz* plane through 8a, 32e, and 16c sites (the same section as that in Figure 5). Contour lines are in steps of 100 meV. The dotted line shows the linear section along the [111] direction depicted in part b.

Structure Evolution with Temperature. As seen from the behavior of the u parameter in Figure 2, the 8a tetrahedral volume increases strongly with the temperature. The volume increase of the 16d octahedron is less, which is due to the stronger Ti−O bond in the octahedron compared with the Li−O bond in the tetrahedron, and thus the Li1−O distance is already becoming larger than the Li2/Ti−O distance ($u > 0.0125$) below 100 °C (Figure 2c). Extrapolation of the isotropic ADPs to 0 K shows that all pass through $B_{iso} = 0$ at 0 K (Figure 2d). This means that no appreciable disorder is present in this compound. Only B_{iso} of Li1 on the 8a site starts to deviate above 700 °C, indicating the onset of anharmonic motion. For this reason, anharmonic refinements have been performed at 900 °C.

Lithium Migration. Regarding, e.g., the recent study by Vijayakumar et al.[18] on a $Li_4Ti_5O_{12}$ sample, one can propose that the lithium occupancy in $Li_4Ti_5O_{12}$ depends on the

dx.doi.org/10.1021/cm103332y |*Chem. Mater.* 2011, 23, 2753–2759

synthesis technique and/or the synthesis temperature. In ref 18, NMR was used to determine that lithium partly occupies the 16c position at room temperature, in contrast to the observations of the present study. Other studies show that the crystallinity of the $Li_4Ti_5O_{12}$ samples strongly depends on the annealing temperature[37] and that the electrochemical intercalation of more than three Li^+ ions in nanoparticulate $Li_4Ti_5O_{12}$ samples is possible.[11] This suggests that the particle size as well as the synthesis conditions influences the crystal structure, and probably also the ionic conductivity and lithium migration in $Li_4Ti_5O_{12}$. In the present study, below 700 °C, the lithium occupancy on crystallographic sites other than 8a and 16d could not be proven. Higher lithium mobility was determined at 700 °C, and lithium migration of approximately 14(2)% from tetrahedral 8a sites to the split sites around 16c is determined at 900 °C. The PDF of lithium on 8a at 900 °C (Figure 5) shows bulges in the directions of the tetrahedral faces, typical for anharmonic vibrations in tetrahedral symmetry. The negative areas in Figure 5 are artifacts due to series termination effects, which usually appear for very large gradients of the PDF. Here they simply demonstrate the repulsion toward the nearest oxygen atom. It has to be noted that the distance between Li* and the nearest oxygen is similar to that between Li1 and oxygen (cf. Table 4), meaning that a transient bond between Li* and oxygen is established (indicated by the connecting lines in Figure 5). Note that Li* exactly on 16c would lead to an unacceptable long distance of about 2.24 Å. Therewith, a plausible diffusion path may be presented. Stimulated by the anharmonic vibration, lithium passes from 8a through the face of the surrounding oxygen tetrahedron to the neighboring Li* site (step 1), switches to the adjacent Li* site (step 2), where it is bonded transiently to another oxygen, and jumps into the next tetrahedron (step 1′). In this way, only rather short jump distances are involved: 1.20, 1.28, and 1.20 Å (cf. Table 4). This process is facilitated by the increase of the tetrahedral volume (see Figure 2c), meaning an enlargement of the opening of the oxygen triangle formed by the tetrahedral face. From Figure 6a,b, the activation energies for steps 1 and 2 are about 500 and 800 meV, respectively. The ADP of Li* being isotropic and constrained to that of Li1 is certainly an oversimplification imposed by the refinement requirements, such that the true activation energies are expected to be somewhat lower. Therewith, they are in good agreement with the experimental value of 640 meV[14] at the same temperature. It should be emphasized that the PDF, as determined by diffraction methods, is a time and space average and is thus comparable to macroscopic measurements. It does not represent an actual single-hopping process, which is triggered by phonon-assisted opening of the "windows". Wagemaker et al.[23] proposed that the 16c position is unoccupied and that there is a saddle point of the energy barrier between the two 8a positions. Although their NMR measurements were done at room temperature and on partially intercalated samples, they can be compared with our findings at high temperatures because the potential landscape imposed by the surrounding framework is still similar. Hence, the results of the present study at 900 °C match nicely with the lithium diffusion path at low temperatures, refining it further by observation on the 32e sites. Similarly, one could propose that the possible lithium occupancy, other than on 8a or 16d, will be on split sites 32e rather than exactly on 16c. Because in using NMR no direct average structure information can be revealed, it might be possible that Vijayakumar et al.[18] observed the signal of the chemical shift of lithium on 32e instead of lithium on 16c.

Theories about the order−disorder phase transformations of $Li_4Ti_5O_{12}$ at high temperatures are based on changes of the conductivity measured by impedance spectroscopy.[13,14] Whether the method to synthesize $Li_4Ti_5O_{12}$ or the measurement conditions for high-temperature experiments influence the results has to be verified. High-temperature measurements were performed either in air or in vacuum, operated with different heating rates, and the constitution of the sample varies by using either pressed pellets[13−16] or a loose powder, as in the present study. Here, neutron powder diffraction was applied to study $Li_4Ti_5O_{12}$ at high temperatures, and no order−disorder phase transition could be observed, except partial lithium migration to split sites around the 16c positions at 900 °C and higher lithium mobility starting at 700 °C.

CONCLUSIONS

The inferred order−disorder phase transitions upon heating of $Li_4Ti_5O_{12}$ cannot be confirmed by the present study. Because of higher lithium mobility above 700 °C, lithium ions start to migrate from the tetrahedral 8a positions but do not reside on 16c sites, as was assumed before. Lithium ions are displaced from the 16c sites into metastable positions determined by a potential minimum imposed by the surrounding oxygen geometry. It has already been shown before using NMR measurements at low temperatures that the 16c sites are unfavorable positions for lithium diffusion, which compares well with our findings for the lithium occupancy and lithium diffusion in $Li_4Ti_5O_{12}$ at high temperatures. The activation energy determined in the present study at 900 °C is in good agreement with the literature. Moreover, neutron powder diffraction is able to reveal the actual details of the long-range three-dimensional zigzag diffusion path in all ⟨110⟩ directions.

ASSOCIATED CONTENT

Supporting Information. Seven CIF files recorded at room temperature (15 °C), 300, 500, 700, 900, 1000, and 1100 °C, created using the program *FULLPROF*,[26] and a CIF file of the 900 °C measurement, created by the program *JANA*.[28] This material is available free of charge via the Internet at http://pubs.acs.org.

AUTHOR INFORMATION

Corresponding Author
*E-mail: laumann@min.uni-muenchen.de.

ACKNOWLEDGMENT

E. Schmidbauer is thanked for fruitful discussions. M.B. thanks the Villum Kann Rasmussen Foundation for funding, and A.L. thanks Süd-Chemie AG for funding.

REFERENCES

(1) Ferg, E.; Gummow, R. J.; De Kock, A.; Thackeray, M. M. *J. Electrochem. Soc.* **1994**, *141*, L147.
(2) Ohzuku, T.; Ueda, A.; Yamamoto, N. *J. Electrochem. Soc.* **1995**, *142*, 1431.
(3) Scharner, S.; Weppner, W.; Schmid-Beurmann, R. *J. Electrochem. Soc.* **1999**, *146*, 857.
(4) Matsui, E.; Abe, Y.; Senna, M.; Guerfi, A.; Zaghib, K. *J. Am. Ceram. Soc.* **2008**, *91*, 1522.

(5) Colbow, K. M.; Dahn, J. R.; Haering, R. R. *J. Power Sources* **1989**, *26*, 397.
(6) Zaghib, K.; Simoneau, M.; Armand, M.; Gauthier, M. *J. Power Sources* **1999**, *81*−*82*, 300.
(7) Deschanvres, A.; Raveau, B.; Sekkal, Z. *Mater. Res. Bull.* **1971**, *6*, 699.
(8) Kataoka, K.; Takahashi, Y.; Kijima, N.; Akimoto, J.; Oshima, K. *J. Phys. Chem. Solids* **2008**, *69*, 1454.
(9) Julien, C. M.; Zaghib, K. *Electrochim. Acta* **2004**, *50*, 411.
(10) Wagemaker, M.; Simon, D. R.; Kelder, E. M.; Schoonman, J.; Ringpfeil, C.; Haake, U.; Lützenkirchen-Hecht, D.; Frahm, R.; Mulder, F. M. *Adv. Mater.* **2006**, *18*, 3169.
(11) Borghols, W. J. H.; Wagemaker, M.; Lafont, U.; Kelder, E. M.; Mulder, F. M. *J. Am. Chem. Soc.* **2010**, *131*, 17786.
(12) Colin, J.-F.; Godbole, V.; Novák, P. *Electrochem. Commun.* **2010**, *12*, 804.
(13) Leonidov, I. A.; Leonidova, O. N.; Perelyaeva, L. A.; Samigullina, R. F.; Kovyazina, S. A.; Patrakeev, M. V. *Phys. Solid State* **2003**, *45*, 2079.
(14) Leonidov, I. A.; Leonidova, O. N.; Samigullina, R. F.; Partrakeev, M. V. *J. Struct. Chem.* **2004**, *45*, 262.
(15) Vitiņš, Ģ.; Ķizāne, G.; Lūsis, A.; Tiliks, J. *J. Solid State Electrochem.* **2002**, *6*, 311.
(16) Fehr, K. T.; Holzapfel, M.; Laumann, A.; Schmidbauer, E. *Solid State Ionics* **2010**, *181*, 1111.
(17) Pecharromán, C.; Amarilla, J. M. *Phys. Rev. B* **2000**, *62*, 12063.
(18) Vijayakumar, M.; Kerisit, S.; Rosso, K. M.; Burton, S. D.; Sears, J. A.; Yang, Z.; Graff, G. L.; Liu, J.; Hu, J. *J. Power Sources* **2011**, *196*, 2211.
(19) Gicquel, C.; Mayer, M. M.; Bouaziz, R. *C. R. Acad. Sci. Paris, Sér. C* **1972**, *275*, 1427.
(20) Izquierdo, G.; West, A. *Mater. Res. Bull.* **1980**, *15*, 1655.
(21) Kleykamp, H. *Fusion Eng. Des.* **2002**, *61*−*62*, 361.
(22) Wilkening, M.; Amade, R.; Iwaniak, W.; Heitjans, P. *Phys. Chem. Chem. Phys.* **2007**, *9*, 1239.
(23) Wagemaker, M.; van Eck, E. R. H.; Kentgens, A. P. M.; Mulder, F. M. *J. Phys. Chem. B* **2009**, *113*, 224.
(24) Aldon, L.; Kubiak, P.; Womes, M.; Jumas, J. C.; Olivier-Fourcade, J.; Tirado, J. L.; Corredor, J. I.; Vicente, C. P. *Chem. Mater.* **2004**, *16*, 5721.
(25) Hoelzel, M.; Senyshyn, A.; Gilles, R.; Boysen, H.; Fuess, H. *Neutron News* **2007**, *18*, 23.
(26) Rodríguez-Carvajal, J. *Physica B* **1993**, *192*, 55.
(27) Thompson, P.; Cox, D. E.; Hastings, J. B. *J. Appl. Crystallogr.* **1987**, *20*, 79.
(28) Petricek, V.; Dušek, M. *The Crystallographic Computing System JANA2000*; Institute of Physics: Praha, Czech Republic, 2000.
(29) Han, T. *International Tables for Crystallography*; Reidel: Dordecht, The Netherlands, 1983; Vol. A.
(30) Kataoka, K.; Takahashi, Y. Y.; Kijima, N.; Nagai, H. *Mater. Res. Bull.* **2009**, *44*, 168.
(31) Laumann, A.; Fehr, K. T.; Boysen, H.; Hoelzel, M.; Holzapfel, M. *Z. Kristallogr.* **2011**, *226*, 53.
(32) Mikkelsen, J. C. *J. Am. Ceram. Soc.* **1980**, *63*, 331.
(33) Boysen, H. *Z. Kristallogr.* **2003**, *218*, 123.
(34) Laumann, A.; Fehr, K. T.; Holzapfel, M.; Wachsmann, M.; Iversen, B. B. *Solid State Ionics* **2010**, *181*, 1525.
(35) Huang, S.; Wen, Z.; Zhu, X.; Gu, Z. *Electrochem. Commun.* **2004**, *6*, 1093.
(36) Yu, Y.; Shui, J. L.; Chen, C. H. *Solid State Commun.* **2005**, *135*, 485.
(37) Qiu, Z.; Yang, L.; Tang, Y.; Fang, S.; Huang, J. *Chin. J. Chem.* **2010**, *28*, 911.